RAD Conference Proceedings, vol. 8, pp. 110-116, 2024
ISSN 2466-4626 (online) | DOI: 10.21175/RadProc.2024.20
www.rad-proceedings.org

# A THREE-DIMENSIONAL CFD-BASED APPROACH FOR THE DISPERSION OF RADIOACTIVE CLOUD IN URBAN ENVIRONMENT

**Giuseppe Giannattasio[1*], Alessio Castorrini[2], Michele Ferrarini[3], Francesco Bonforte[3], Antonio D'Angola[1]**

[1]Dipartimento di Ingegneria - Università degli Studi della Basilicata, Potenza, Italy
[2]Dipartimento di Ingegneria Meccanica e Aerospaziale - Sapienza Università di Roma, Rome, Italy
[3]Fondazione CNAO, Pavia, Italy

**Abstract**. *The presence of buildings and obstacles in urban environment can modify the velocity and spatial concentration fields of gaseous pollutants emitted by a source, therefore affecting the dispersion of the plume. The dispersion of the pollutants can be analytically approximated by using Briggs' coefficients limited by the lack of detailed geometrical information of the obstacles.*
*In the work, similarity Theory (MOST) for the entire vertical Atmospheric Boundary Layer profile under non-neutral stability conditions has been included as an accurate inlet boundary condition in the framework of the Reynolds-Averaged Navier-Stokes (RANS) approach. The effectiveness of the Shear Stress Transport (SST) variant of the k-ω model has been highlighted as the appropriate turbulence closure model to be used for the dispersion of cloud in urban environment.*
*The geometry used in the numerical simulation was inspired by an urban agglomeration and refinement regions were strategically set to accurately capture the flow field and plume transport near obstacle surfaces, close to the ground, and around the chimney. Comparisons between Gaussian plume and CFD-based models are reported showing differences and asymmetries especially at shorter distance. Numerical results have been obtained by considering different stability atmospheric conditions and comparisons and differences with Huber approximation are presented and discussed.*

**Keywords***: Turbulence, Gaussian Plume Model, Huber's Theory, Computational Fluid Dynamics, Radioactive clouds, Atmospheric Boundary Layer, Atmospheric Stability, Monin-Obukhov Similarity Theory*

## 1. Introduction

Given the environmental impact assessment criteria imposed by the current legislation on population safety and prevention, research on the dispersion of gaseous contaminants into the atmosphere in the vicinity of metropolitan centers is becoming increasingly relevant. The health effects are then clearly linked to the kind of pollutants, which are typically a source of chemical risk but also of ionizing radiation from radioactive materials. For instance, this can happen as a result of the cycles of the particle acceleration equipment used in oncological treatment therapy centers, which are typically located close to urban areas [1-3]. In this case, the plume emitted by the chimney is typically composed by a mixture of short life β+ emitters and Argon-41 (gamma emitter). In order to assess regulatory criteria, dispersion of gaseous contaminants is typically evaluated by recurring to simplified analytical models, such as the Gaussian Plume Model (GPM), both in open and urban environment. The models allow the user to select from a wide variety of parameters (chimney height, wind speed, atmospheric stability class) and are adaptable to different conditions.

Due to the approximations in GPM at short distances, more accurate fluid dynamic simulations can be performed in order to overcome the approximation given by the GPM especially at short distances from the chimney. CFD simulations can be very useful when there are obstacles and structures in the region of plume convection and can precisely characterize the impact of complex geometries on the turbulent wind field, which is related to atmospheric conditions and local recirculation. Among various CFD models, Reynolds Averaged Navier-Stokes equations (RANS) typically provide a good approximation of the turbulent wind field at a sustainable computational cost [2, 4, 5]. Therefore, CFD-based approaches might be suitable for urban areas in which results obtained by simplified models could be affected by approximations that might results assuming an open and unhindered field.

In the present paper, transport phenomena of gaseous pollutants in urban environment have been investigated in turbulent regime by using a CFD approach with improved inlet boundary conditions. Accuracy of the results is sensitive to the selected parameters, and the effectiveness of the Shear Stress Transport (SST) variant of the k-ω model [5] coupled with the MOST theory for the inlet boundary condition has been established as the most

* E-mail of the corresponding author – giuseppe.giannattasio@unibas.it

appropriate turbulence closure model to investigate dispersion in urban environment.

The paper presents the following structure: in Section 2, the GPM model with Huber corrections have been described; in Section 3 the theory of Monin-Obukhov have been introduced while in Section 4 numerical results have been reported and discussed along with comparison with the GPM model.

## 2. Gaussian plume equation

### *2.1. General model and Huber's correction*

The following formula provides the typical Gaussian Plume equation used in Pasquill's theory to evaluate the concentration $C(x,y,z)$ of a gas or air pollutant emitted by a source:

$$C = \frac{Qe^{-\frac{y^2}{2\sigma_y^2}}}{2\pi u\sigma_y\sigma_z}\left[e^{-\frac{(z-H_s)^2}{2\sigma_z^2}} + e^{-\frac{(z+H_s)^2}{2\sigma_z^2}}\right] \quad (1)$$

where $x$ represents the distance from the source in the direction of the wind, $y$ and $z$ along the transverse directions ($z$ is the height from the ground), $H_s$, $Q$, $u$, $\sigma_z$, $\sigma_y$ are the effective source height, the continuous source emission rate of the pollutant, the mean transport wind velocity in the direction of the $x$ axis and the diffusion parameters in the corresponding directions, respectively [6-8]. Gaussian distributions of the pollutant in the direction corresponding to the plume's drift can be found as the analytical solution of a simplified diffusion equation. For the dispersion diffusion parameters, many models can be used, either in open fields or with the impact of buildings included. The following expressions, which are commonly used, provide Briggs' coefficients as a function of the distance by the source $x$:

$$\sigma_y = a\cdot x\cdot(1+c\cdot x)^{-0.5} \qquad \sigma_z = a\cdot x\cdot(1+c\cdot x)^{d} \quad (2)$$

where $a$, $c$ and $d$ are coefficients which depend on the surroundings and the stability class of the atmosphere. GPMs prove to be effective at long distance from the source but could be affected by unacceptable errors at lower distance.

Regarding the spreading of the plume due to the presence of buildings near the source, Huber's theory considers the solution independent from environmental turbulence in the range $3H_b$ - $10H_b$, where $H_b$ is the height of the highest building close to the emitting source. For $x > 10H_b$, Huber model no longer depends on the presence of obstacles but only on the environmental turbulence. The following equations (3-4) show Huber's corrections of dispersion parameters $\sigma^H$ in the presence of buildings

$$\sigma^H{}_y = [\sigma^2{}_y + (0.7W_b/2)^2]^{0.5} \quad (3)$$

$$\sigma^H{}_z = [\sigma^2{}_z + (0.7H_b/2)^2]^{0.5} \quad (4)$$

where $\sigma^H$ is the dispersion parameter function of the distance $x$ from the source in the horizontal direction of the wind and $W_b$ is the width of the region of influence orthogonal to wind.

Equations (3) and (4) are valid for $x > 3H_b$ but it is possible to estimate dispersion parameters in the presence of obstacles in range 0-3 $H_b$ setting $x = 3H_b$ [9, 10]. A comparison between Pasquill and Huber results are reported in Section 4 after the introduction of the MOST theory, given in Section 3.

## 3. The Monin-Obukhov similarity theory

An accurate resolution of the Atmospheric Boundary Layer profile (ABL) in a RANS simulation requires the definition of appropriate and consistent boundary conditions for velocity, turbulence, and temperature. The Monin-Obukhov Similarity Theory (MOST) is commonly used to account for different stability conditions in the atmospheric surface layer [11]. According to the MOST theory, it is possible to derive the following vertical profiles to be applied as boundary conditions for the Reynolds averaged velocity $u(z)$, potential temperature $\vartheta(z)$, turbulent kinetic energy $k(z)$ and dissipation rate $\varepsilon(z)$, with $z$ being the distance from the ground.

The equations (5-8) for the profiles of the aforementioned quantities according to the MOST theory are the following [10]

$$u(z) = \frac{u_*}{\kappa}\left[\ln\left(\frac{z}{z_0}\right) - \psi_m\left(\frac{z}{L}\right)\right] \quad (5)$$

$$\vartheta(z) = \vartheta(z_0) + \frac{\vartheta_*}{\kappa}\left[\ln\left(\frac{z}{z_0}\right) - \psi_t\left(\frac{z}{L}\right)\right] \quad (6)$$

$$k(z) = \frac{u_*^2}{\sqrt{C_\mu}}\psi_k\left(\frac{z}{L}\right) \quad (7)$$

$$\varepsilon(z) = \frac{u_*^3}{\kappa z}\psi_\varepsilon\left(\frac{z}{L}\right) \quad (8)$$

being $\psi_k = \sqrt{\psi_\varepsilon/\psi_m}$ and where $z_0$ is the roughness parameter, $u_*$ is the friction velocity, $\kappa$ is the Von Karman constant, $L$ is the Monin Obukhov Length, $\vartheta_*$ is temperature length scale, $C_\mu$ is a turbulence model constant and the functions $\psi$ are the stability-related functions defined by the MOST theory *according to atmospheric stability classes*.

Using the MOST theory, it is possible to provide wind and temperature profiles at the inflow boundary of the computational domain, which are based on the Pasquill stability classes. The values can be also adopted as reference to compute the analytic concentration with GPM. In order to make comparisons between Pasquill, Huber and CFD results, the spatial distribution of the velocity field is taken into account in the processing of the simulation

results [12]. A detailed discussion has been reported in Sections 4 and 6.

## 4. Analytical comparisons

Analytical models used for evaluating the dispersion of pollutants are limited by two main factors: an averaged wind velocity respect to a not uniform spatial velocity distribution and the simplified approach in the presence of obstacles in urban area. Despite these assumptions, analytical approaches are widely adopted especially to respect regulatory constraints. In fact, analytical models are characterized by their excessive sensitivity to the choice of wind velocity value and, regarding the presence of obstacles in urban area, the use of simplified Briggs parameters does not catch the effects of turbulence. CFD simulations overcome these assumptions by calculating accurate velocity and concentration fields.

In this Section, analytical Argon concentration distributions have been reported for the stability class E (slightly stable conditions) at $x$ = 400 m from the source (chimney emitting air/Argon mixture with 5% Ar-mass fraction). The vertical velocity outlet from the chimney is 1 m/s. Since the Gaussian concentration depends on wind velocity and Briggs' parameters, a comparison is shown between the results of Pasquill and Huber expressions for different choices of these parameters.

In fact, in GPM models, some assumptions are considered: the prevailing component of the wind velocity field is horizontal ($x$-direction) and it is considered uniform and constant for a sufficiently long timespan. In real situations, the plume will be inserted a velocity field which is not uniform, the hypothesis of constant speed could be not be verified and an average value should be considered.

Moreover, Briggs' coefficients depend strongly on the surroundings, but in real situation urban areas could present different characteristics and an intermediate value between pure open range and urban value should be considered. For these reasons analytical GPM values have been reported for different values of average wind velocity and for different surroundings. Figures 1 and 2 show the concentration of the pollutants along $y$- and $z$- directions in correspondence of the concentration maximum value ($x$=400m). Results show that surrounding characteristics affect strongly the spatial concentration and a proper value of parameters $a$, $c$ and $d$ for the case under investigation should be considered in Eqs. (2)-(4). In this paper, Briggs parameters were adjusted to modulate the theoretical open-urban range in order to consider the presence of few buildings in the geometry under consideration and the arithmetic means of $a$, $c$ and $d$ respect to full open and full urban conditions have been considered ("0.5 range open-urban").

Similarly, in order to make consistent comparisons between analytical values given by the GPM models and CFD numerical values, a proper value of the wind velocity should be considered in GPM models. These values have been obtained by considering the $x$ component of the 3D velocity distribution evaluated by the CFD model. In fact, the plume is not transported by a single velocity but by a distribution of velocity, which represents one of the limitations of the use of GPM.

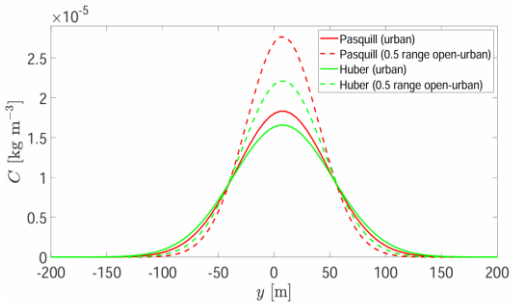


Figure 1. Argon concentration along y direction for stability class E (x = 400 m).

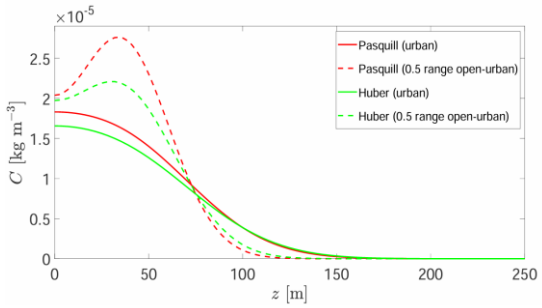


Figure 2. Argon concentration along z direction for stability class E (x = 400 m).

Figures 3 and 4 show the spatial distribution of the pollutant concentration along $y$ and $z$ (in correspondence of its maximum and at a distance $x$=400 m from the source) for different values of the wind velocity in the range [1, 2.8] m/s. The value of 2.8 m/s has been selected being the velocity of the wind at the inlet boundary at the height of the chimney for stability class E.

Results show that spatial concentrations are strongly affected by the wind velocity and in a real case, even if the wind far from the source respect the MOST predicted value, the presence of buildings could affect the spatial distribution of the wind velocity field in which the pollutants are emitted. In this case, a proper averaged value of the wind velocity should be considered in order to carry out consistent comparison between numerical CFD results and analytical values given by GPM. In fact, in Section 6, numerical CFD results show that, for the case under investigation, due to the presence of buildings, wind speed fields are less intense than those introduced by the MOST theory in the inlet boundary condition. By assuming lower values of the averaged wind velocity, results show that Pasquill/Huber concentrations are

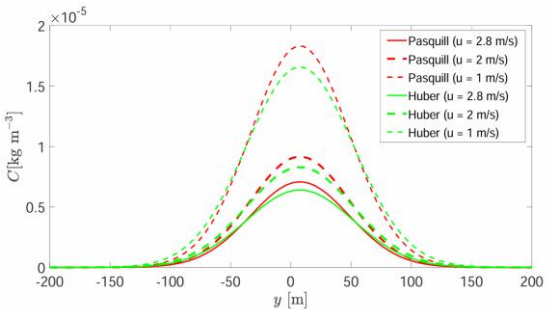


Figure 3. Argon concentration along y direction for stability class E at x = 400 m depending on the wind velocity parameter

numerical ones. Hence, with the analytical curves, generally prevailing over the numerical ones in relation to the maximum values, GPM models, even with the Huber corrections, overestimate the environmental doses due to a lower dilution of the air contaminant. Starting from spatial distributions, dose values coming from ionizing radiation can be obtained recurring to appropriate conversion factors [13].

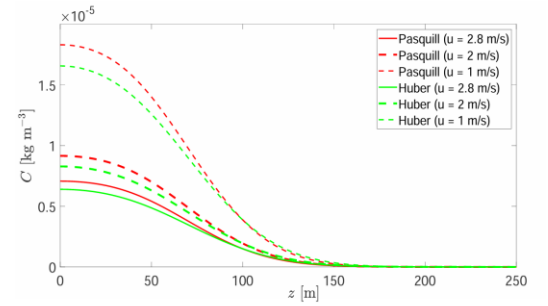


Figure 4. Argon concentration along z direction for stability class E at x = 400 m depending on the wind velocity parameter

## 5. Geometry and CFD model setting

The computational domain under investigation is a 3D rectangular prism with $L_x$=1.3 km, $L_y$=0.75 km and $L_z$=0.5 km. In the domain, a squared chimney (height $h$=3.1 m and side $l$=1.5 m) is placed above the roof of a building of height $H$=20 m and width $W$=115 m. The coordinates of the center of the chimney outlet are $x$=59.35 m, $y$=7.6 m and $z$=0 m.

An unstructured hybrid mesh with local refinement regions has been generated to solve the plume transport region and the flow field close to the ground, to the buildings and to the chimney. Two Body of Influence (BOI) has been considered in order to increase the mesh resolution near the buildings (green boxes in Figs. 5 and 6): a cylinder with radius $R$ = 35 m and length $l_1$=156 m to obtain a finer meshing in correspondence of the plume emission from the chimney and a box with length $l_2$ = 193 m, height $l_3$ = 60 m and width $l_4$ = 175 m to improve resolution when the plume moves towards the ground. The chosen calculation grid was validated with a grid sensitivity analysis. Finally, we selected $6.2 \cdot 10^6$ cells for the full domain while element sizes of 2 m and 4 m for cylindrical and rectangular BOIs, respectively.

The model has been implemented in the framework of Ansys Academic Research CFD 2023 R1 [12, 14] with boundary conditions types reported in Table 1.

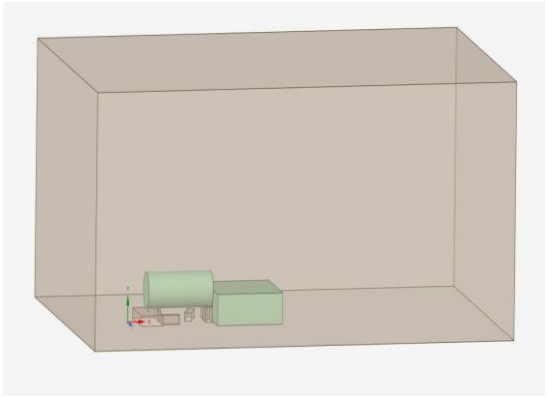

Figure 5. Real geometry with BOI

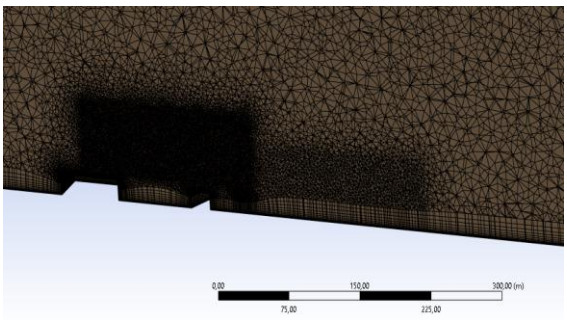

Figure 6. Mesh section on xz plane

Table 1. Boundary conditions of the domain

| Face | Type |
|---|---|
| Inlet_chimney | *velocity_inlet* |
| Inlet_wind | *velocity_inlet* |
| Outlet_wind | *outflow* |
| Outlet_sides | *symmetry* |
| Farfield_upper | *velocity_inlet* |
| Bottom surface | *wall* |

## 6. Numerical results

Numerical results have been obtained by considering Class E stability (slightly stable conditions) and considering an urban surroundings case [15]. Comparisons between the Gaussian Plume Model (Pasquill-Huber) and CFD-based model [11]

are presented and discussed. Numerical concentrations of Argon have been gathered on four planes orthogonal to wind direction ($x$) and placed at downstream distance $x$ = 50 m, 100 m, 200 m and 400 m from the chimney position. The results at distance $x$ = 50 m and 100 m are shown in Figures 7-10. Due to the asymmetries introduced by the real domain, numerical values obtained by the CFD simulations will be characterized, at different $x$-distances, by an offset respect to the position of the chimney in the $yz$ plane, and, consequently, the maximum value of the spatial concentration will be located far from the maximum value obtained by GPM models, in which the asymmetry is not considered. For this reason, results will be presented along $y/(z)$-direction in correspondence of the $z/(y)$-value in which the maximum of the 2D concentration is obtained both for GPM model ("max Analytical") and CFD ("max CFD").

Figures 7 and 8 (in max Analytical) show the comparison of the spatial distributions of the concentrations when the maximum value is obtained in the GPM model. Results confirm the offset along $z$ of the CFD distribution respect to the GPM case, even if the maximum values of the concentration are in good agreement ($3.1 \cdot 10^{-4}$-$3.3 \cdot 10^{-4}$ kg/m$^3$).

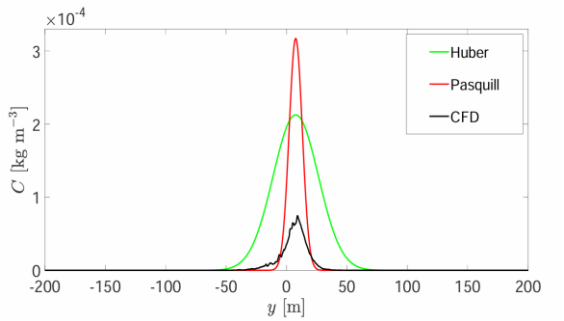


Figure 7. Concentration at x = 50 m along y (z = 35.7 m)

In Figures 7 and 8, the wind velocity $u$ = 2.8 m/s (in correspondence of the chimney height) has been considered equal to the inflow value obtained with MOST theory [16]. In order to consider the effect of the spatial distribution of the wind velocity [17-19] in GPM expressions, the analytical curves of Pasquill and Huber are represented with different $u$ values and compared with CFD results. In fact, the $x$-component of the velocity can be strongly affected by the presence of the buildings and can assume lower values respect to the inlet value ($u_{inlet}$=2.8 m/s). Figures 9 and 10 show the CFD spatial distribution of the $x$ component of the velocity fileld on the $yz$ plane at $x$=50 and 100 m, respectively. The velocity is strongly reduced (1 m/s) respect to its inlet value at boundaries (2.8 m/s) and, due to the presence of buildings, can assume negative value due to the recirculation.

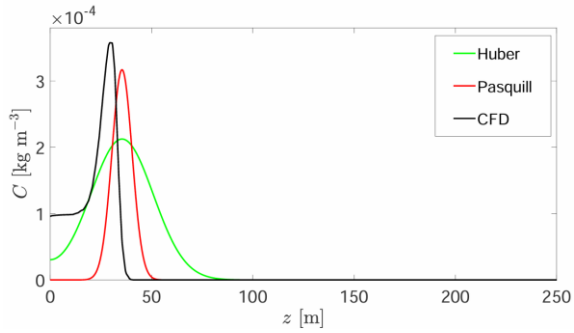


Figure 8. Concentration at x = 50 m along z (y = 7.5 m)

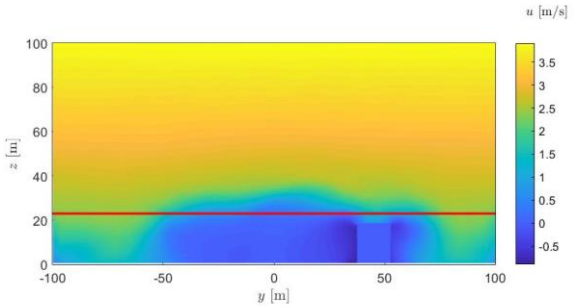


Figure 9. x component of the velocity filed on the yz plane at x=50 m. Red line is located at the z position of the chimney

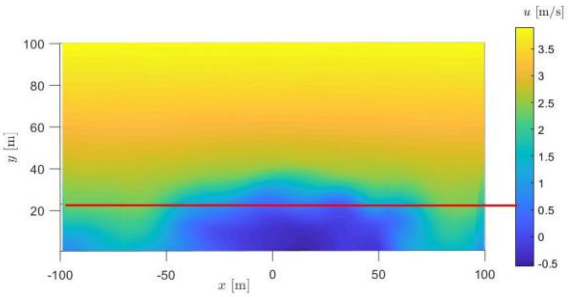


Figure 10. x component of the velocity field (u) on the yz plane at x=100 m. Red line is located at the z position of the chimney

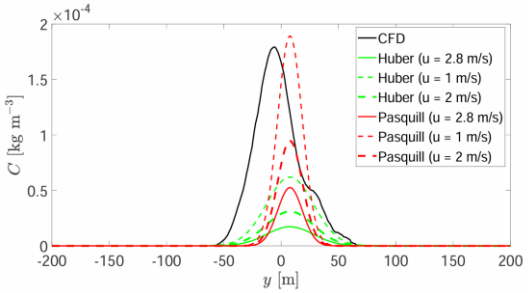


Figure 11. Concentration at x = 100 m along y (z = 27.0 m)

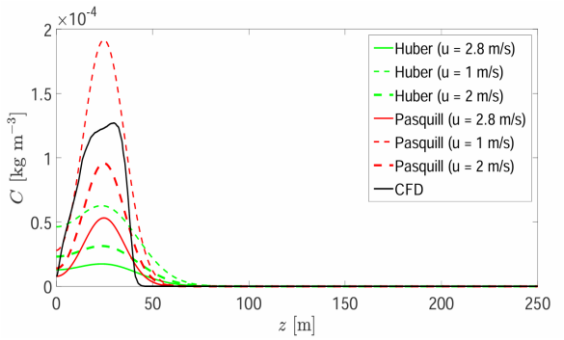


Figure 12. Concentration at x = 100 m along z (y = 7.5 m)

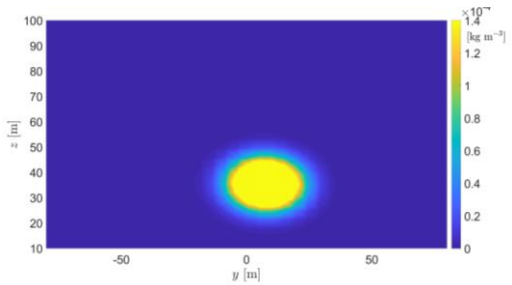


Figure 14. Pasquill concentration (2D)

Taking into account these corrections, numerical solutions, compared to analytical ones, show a higher dilution of the contaminant in the atmosphere with a much lower environmental dose forecast. Results are reported in Figures 11 (in max CFD) and 12 (in max Analytical) and highlight that, in order to make a consistent comparison between analytical and CFD results, a proper average value of the wind velocity should be considered in the analytical expressions. In fact, in the case of $u$=1 m/s, Pasquill distribution prevails over the numerical ones in relation to the maximum values and overestimates the environmental doses due to a lower dilution of the air contaminant. Finally, numerical CFD results confirm the asymmetry introduced by the presence of the buildings as shown in Figures 13 and 14, in which the 2D concentrations are reported in cross-sectional view of the wind direction at $x$=100 m from the chimney. The numerical CFD distribution is scattered because of the presence of buildings that hinder the Argon plume. The analytical concentration (Pasquill) following the simplified GPM model is much more regular. The accuracy of the results will be improved by incorporating in the future high-resolution urban topographic data of the case under investigation.

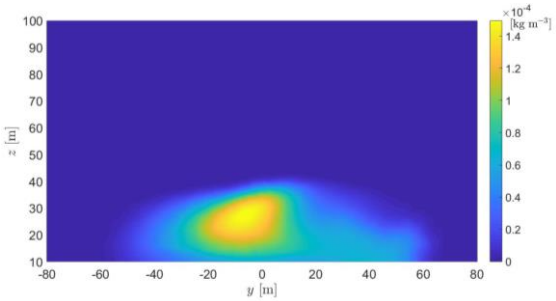


Figure 13. CFD concentration (2D)

## 7. Conclusions

Air pollution is considered one of the largest environmental health risk and, for this reason, the choice of an appropriate modeling framework is essential to accurately calculate air pollution dispersion and its healthy consequences. Buildings and other obstacles in an urban setting can alter the velocity and spatial concentration fields of pollutant contaminants released by a source, which can impact the plume's dispersion. An analytical calculation of the pollutant dispersion is made using Briggs' coefficients, which depend on weather factors, including wind speed and air stability. The lack of precise geometrical details of the obstacles is one of the model's limit, leading to a simplified representation of the spatial distribution of the radioactive cloud's concentration and velocity around the source.

The practical implication of this study regards the necessity of implementing CFD model and adequate boundary conditions to predict dispersion in urban area in which turbulence phenomena affects spatial distribution of the concentration.

In the paper, the CFD approach selected is characterized by:

- the implementation of the Shear Stress Transport (SST) variant of the k-ω model in the framework of Reynolds-Averaged Navier-Stokes (RANS) approach;
- the implementation of a high resolution grid validated with sensitivity analysis introducing Body Of Influence (BOI) geometries;
- the use of the similarity Theory (MOST) for the entire vertical Atmospheric Boundary Layer profile under non-neutral stability conditions.

Comparisons with simplified Gaussian analytics expressions highlight differences especially at shorter distance. Results show that analytical representations could be strongly affected by the hypotheses of constant and uniform wind velocity and by the presence of buildings. For these reasons more accurate CFD results are suggested. Future developments will take into account thermal gradient of the air and, in the case of a radioactive source, an accurate evaluation of the dose by recurring to Monte Carlo codes [20, 21].

## References

1. M. Pantusheva, R.Mitkov, P.O. Hristov, D. Petrova-Antonova, “Air Pollution DispersionModelling in Urban Environment Using CFD: A Systematic Review”, *Atmosphere,* vol. 13, 1640, 2022. https://doi.org/10.3390/atmos13101640
2. Y. Kong, J. Zhang, S. Zhang, Y. Jiang, B. Wang, “CFD Numerical Simulation of Wind Field and Pollutant Dispersion in Valley Cities”, *Gansu Key*

*Laboratory, Lanzhou University, Northwest Regional Climate Center*.
3. M. Pullia, "Status report on the centro nazionale di adroterapia oncologica (cnao)", *IEEE Trans. Appl. Supercond.*, vol. 16, no. 2, pp 1708–1711, 2006. https://doi.org/10.1007/978-981-19-9822-5_5
4. P.J Richards, R.P Hoxey, "Appropriate boundary conditions for computational wind engineering models using the k-ϵ turbulence model", *J. Wind Eng. Ind. Aerodyn.*, vol. 46–47, pp. 145-153, 1993. https://doi.org/10.1016/0167-6105(93)90124-7
5. F.R. Menter, M. Kuntz, R. Langtry, "Ten years of industrial experience with the SST turbulence model", *Turbul Heat Mass Transf*, 2003. Retrieved from: https://www.researchgate.net/publication/228742295_Ten_years_of_industrial_experience_with_the_SST_turbulence_model
6. F. Pasquill, "Atmospheric Diffusion", John Wiley and Sons, New York, 1974.
7. G.A. Briggs, "Diffusion Estimation for Small Emissions", *Air Resources Atmospheric Turbulence and Diffusion Laboratory, NOAA Oak Ridge, Tennessee*. G.A. Briggs, Preliminary report, United States. https://doi.org/10.2172/5118833
8. G.A. Briggs, "Plume rise and buoyancy effects, Atmospheric Science and Power Production", ed. Randerson D., DOE/TIC 27601, Springfield, Department of Commerce, USA, 1984.
9. A.H. Huber, "Evaluation of a method for estimating pollution concentrations downwind of influencing buildings", *Atmos. Environ.*, vol. 18, no. 11, pp. 2313-2338, 1967. https://doi.org/10.1016/0004-6981(84)90003-9
10. A.H. Huber, W.H. Snyder, "Buildings wake effects on short stack effluents", *Reprint Volume for the Third Symposium on Atmospheric Diffusion and Air Quality*, AMS, 1976.
11. A.S. Monin, A.M. Obukhov, "Basic laws of turbulent mixing in the surface layer of the atmosphere", Originally published in *Tr. Akad. Nauk SSSR Geophiz. Inst.*, vol. 24, no. 151, pp. 163-187, 1954. Retrieved from: https://gibbs.science/efd/handouts/monin_obukhov_1954.pdf
12. Ansys® ANSYS FLUENT 12.0 User's Guide, 7.3.2 Using Flow Boundary Conditions release 12.0, ©ANSYS.Inc. 2009-01-29.
13. "Screening Models for Releases of Radionuclides to Atmosphere, Surface Water", and Ground, NCRP Report No. 123 I, 1996.
14. G. Giannattasio, A. Castorrini, A. D'Angola, M. Ferrarini, F. Bonforte, "Three-dimensional Computational Fluid Dynamics investigation of the dispersion of radioactive cloud", *RAD Conf. Proc.*, vol. 7, pp. 79-85, 2023. https://doi.org/10.21175/radproc.2023.15
15. A. Sogachev, M. Kelly, M.Y. Leclerc, "Consistent two-equation closure modeling for atmospheric research: buoyancy and vegetation implementations", *Bound-Lay Meteorol*,, vol. 145, no. 2, pp. 307–327, 2012. https://doi.org/10.1007/s10546-012-9726-5
16. A. Castorrini, S. Gentile, E. Geraldi, A. Bonfiglioli, "Investigations on offshore wind turbine inflow modelling using numerical weather prediction coupled with local-scale computational fluid dynamics", *Renewable Sustainable Energy Rev.*, vol. 171, 113008 2023. https://doi.org/10.1016/j.rser.2022.113008
17. A.J. Dyer, "A review of flux-profile relationships", *Boundary-Layer Meteorol.*, vol. 7, pp. 363–372, 1974. https://doi.org/10.1007/BF00240838
18. D. Golder, "Relations among stability parameters in the surface layer", *Boundary Layer Meteorology*, vol. 3, pp. 47–58, 1972. https://doi.org/10.1007/BF00769106
19. M. Carestia et al., "Use of the "Hotspot" code for safety and security analysis in Nuclear Power Plants: A Case Study", *Environ. Eng. Manage. J.*, vol. 15, no. 4, pp. 905-912, 2016. https://doi.org/10.30638/eemj.2016.098
20. F. Bonforte, M. Ferrarini, A. D'Angola, E. Giroletti, D. Introini, "Heavy-ions shielding data for hadrontherapy application with Monte Carlo methods", *Radiat. Prot. Dosim.*, vol. 199, no. 17, pp. 2061–2075, 2023. https://doi.org/10.1093/rpd/ncad207
21. T. Lorenzon, F. Bonforte, L. Codispoti, S. Agosteo, M. Ferrarini, "Monte Carlo implementation of a Gaussian plume model for submersion dose calculation at short downwind distances", *Radiat. Prot. Dosim*, vol. 201, no. 1, pp. 41-47, 2024. https://doi.org/10.1093/rpd/ncae218